This article was downloaded by:
On: *29 January 2011*
Access details: *Access Details: Free Access*
Publisher *Taylor & Francis*
Informa Ltd Registered in England and Wales Registered Number: 1072954 Registered office: Mortimer House, 37-41 Mortimer Street, London W1T 3JH, UK

Supramolecular Chemistry
Publication details, including instructions for authors and subscription information:
http://www.informaworld.com/smpp/title~content=t713649759

Hydrogen bond-stabilised *N*-alkylammonium resorcinarene halide cavitands

N. Kodiah Beyeh[a]; Mario Cetina[a]; Miika Löfman[a]; Minna Luostarinen[a]; Alexander Shivanyuk[a]; Kari Rissanen[a]
[a] Department of Chemistry, NanoScience Center, University of Jyväskylä, Jyväskylä, Finland

First published on: 17 November 2010

To cite this Article Beyeh, N. Kodiah , Cetina, Mario , Löfman, Miika , Luostarinen, Minna , Shivanyuk, Alexander and Rissanen, Kari(2010) 'Hydrogen bond-stabilised *N*-alkylammonium resorcinarene halide cavitands', Supramolecular Chemistry, 22: 11, 737 — 750, First published on: 17 November 2010 (iFirst)
To link to this Article: DOI: 10.1080/10610278.2010.506543
URL: http://dx.doi.org/10.1080/10610278.2010.506543

PLEASE SCROLL DOWN FOR ARTICLE

Full terms and conditions of use: http://www.informaworld.com/terms-and-conditions-of-access.pdf

This article may be used for research, teaching and private study purposes. Any substantial or systematic reproduction, re-distribution, re-selling, loan or sub-licensing, systematic supply or distribution in any form to anyone is expressly forbidden.

The publisher does not give any warranty express or implied or make any representation that the contents will be complete or accurate or up to date. The accuracy of any instructions, formulae and drug doses should be independently verified with primary sources. The publisher shall not be liable for any loss, actions, claims, proceedings, demand or costs or damages whatsoever or howsoever caused arising directly or indirectly in connection with or arising out of the use of this material.

Supramolecular Chemistry
Vol. 22, Nos. 11–12, November–December 2010, 737–750

Taylor & Francis
Taylor & Francis Group

Hydrogen bond-stabilised *N*-alkylammonium resorcinarene halide cavitands‡

N. Kodiah Beyeh, Mario Cetina, Miika Löfman, Minna Luostarinen, Alexander Shivanyuk† and Kari Rissanen*

Department of Chemistry, NanoScience Center, University of Jyväskylä, P.O. Box 35, 40014 Jyväskylä, Finland

(*Received 10 May 2010; final version received 13 June 2010*)

A family of hydrogen bond-stabilised *N*-alkylammonium resorcinarene chloride and bromide cavitands were synthesised and characterised with ^{1}H NMR and ESI mass spectrometry. The seven compounds exhibit interestingly either self-inclusion or guest complexation in the solid state evidenced by single crystal X-ray diffraction. The four dimers show self-inclusion of the upper rim propyl chains and consist of two hydrogen-bonded resorcinarene tetracations and six halide anions, while the remaining two halide anions are located in between the dimers linking them via hydrogen bonding. Small solvent molecules such as dichloromethane, methanol, *n*-butanol or chloroform are complexed into the resorcinarene cavity in three 1:1 or 1:2 host–guest complexes. While included, the methanol and butanol molecules are simultaneously hydrogen bonded to the halide anion enhancing the complex formation. The complementary self-inclusion results in a nearly perfect cone conformation of the resorcinarene core in the dimers, while the host–guest complexes are much more distorted.

Keywords: resorcinarenes; tetrabenzoxazines; ammonium halides; hydrogen bonding; X-ray structure

Downloaded At: 14:39 29 January 2011

Introduction

The presence of free hydroxyl groups involved in strong intramolecular hydrogen bonding is critical in the cyclisation step during the synthesis and subsequently maintaining the cone conformation of resorcinarenes (*1*). The disruption of the intramolecular hydrogen bonds leads to the collapse of the unique cone conformation. Considerable interest has been focused on the design and synthesis of calixarenes as biomimetic receptors (*2*). In order to achieve convergent arrangement of binding sites, many of these receptors have utilised the cone shape of the resorcinarenes for a variety of applications (*2*). The easy large-scale preparations of resorcinarenes make them very attractive building blocks in supramolecular chemistry (*3*). Resorcinarenes easily form molecular assemblies via hydrogen bonds such as in the formation of open inclusion complexes (*4*), dimers (*5*), hexamers (*6*) and tubular assemblies (*7*) with cavities aimed at trapping cationic (*4–6*), neutral (*8*) or anionic (*9*) guests.

Functionalisation of resorcinarenes at the aromatic ring via Mannich condensation to form tetrabenzoxazines is widely reported (*10*). The cleavage of tetrabenzoxazines by mineral acids leads to the formation of *N*-alkylammonium resorcinarene halides with strong circular hydrogen bond belt $(\cdots NR_2H_2^+\cdots X^-\cdots NR_2H_2^+\cdots X^-\cdots)_2$ between the ammonium moieties and halide anions leading to water-soluble extended cavitand-like structures (*11*). The use of amino acid derivatives such as phenylalanine in the synthesis of tertiary amine resorcinarene derivatives can lead to a formation of self-complementary dimeric homo- or heterochiral capsules encapsulating highly polar guests (*12*).

Herein, we present the synthesis of several *N*-alkylammonium resorcinarene chlorides and bromides and the structural study of the self-assembly properties of seven of them in the solid state by single crystal X-ray diffraction. We specifically pay attention to the inclusion properties of these compounds and not to their packing. The structures in solution were verified by ^{1}H NMR spectroscopy. Electrospray ionisation (ESI) mass spectrometry is used to study their fragmentation behaviour in the gas phase.

Results and discussion

Synthesis and NMR characterisation

Mannich condensation of resorcinarenes with primary amines in the presence of excess formaldehyde gives the corresponding tetrabenzoxazines in high yields. The tetrabenzoxazines can easily be cleaved by refluxing in the presence of concentrated HCl or HBr in *n*-butanol to give the *N*-alkylammonium resorcinarene halides in yields ranging from 40 to 90% (Scheme 1) (*11*).

The ^{1}H NMR spectra of the *N*-alkylammonium resorcinarene halide cavitands show the compounds to

*Corresponding author. Email: kari.t.rissanen@jyu.fi

†Present address: Enamine Ltd, 23 Alexandra Matrosova Street, 01103 Kiev, Ukraine.

‡Dedicated to the memory of Prof. Dmitry Rudkevich.

ISSN 1061-0278 print/ISSN 1029-0478 online
© 2010 Taylor & Francis
DOI: 10.1080/10610278.2010.506543
http://www.informaworld.com

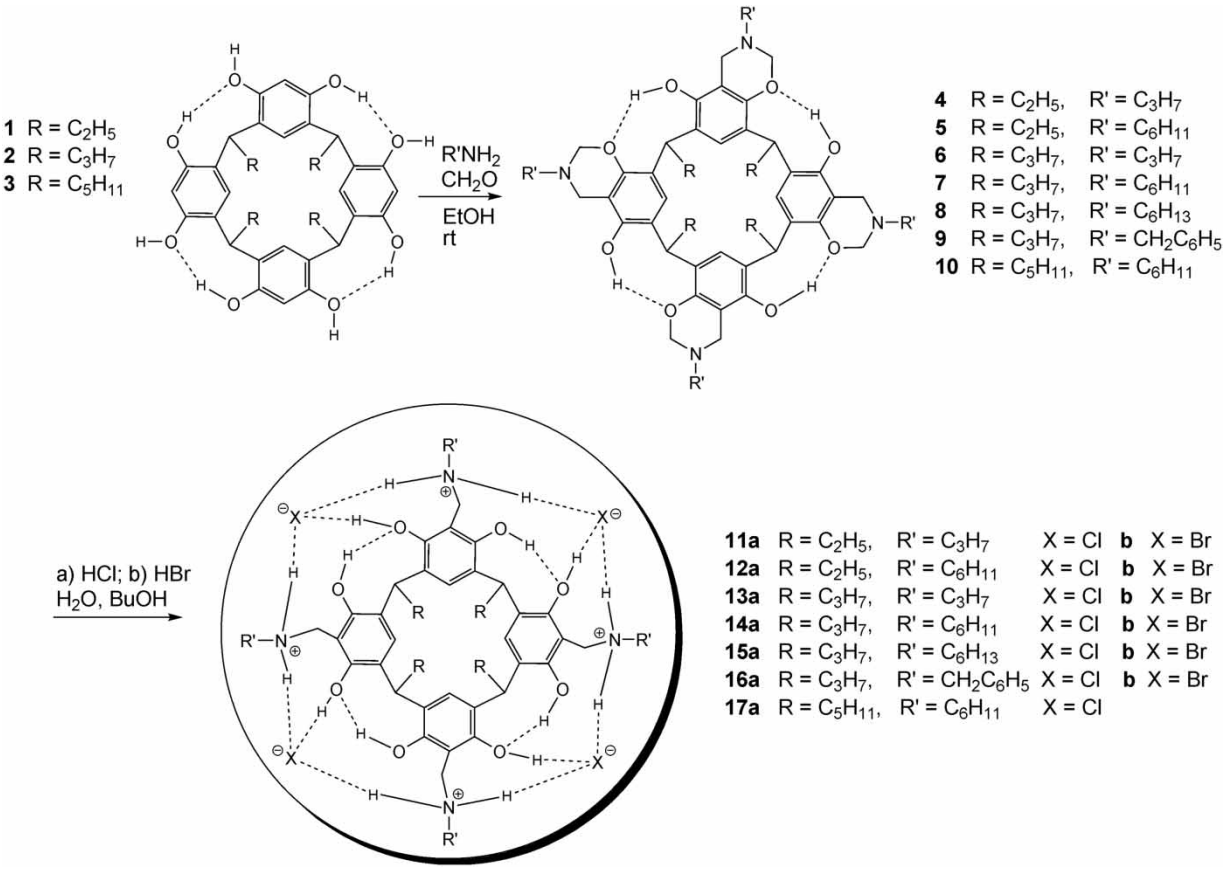

Scheme 1. Synthesis of the resorcinarene tetrabenzoxazines and the corresponding *N*-alkylammonium resorcinarene halide cavitands.

Downloaded At: 14:39 29 January 2011

be relatively symmetrical in solution (*11a*). Taking **14a** in $CDCl_3$ as an example, the proton signals corresponding to the resorcinarene skeleton appear as sharp signals in accordance with a C*4v* symmetrical structure. The methine protons of the resorcinarene scaffold appear around 4.34 ppm as a triplet. The diastereotopic protons of the Ar—CH_2—N group are easily identified as a broad signal at 4.20 ppm. Two different broad peaks corresponding to the hydroxyl and the NH_2^+ groups appear at 8.95 and 7.28 ppm, respectively (Figure 1).

Mass spectrometric analysis

The *N*-alkylammonium resorcinarene halides **11–17** can be easily ionised in the gas phase by ESI mass spectrometric technique using $CHCl_3$/methanol as the spray solvent (*13*). Taking **14b** as an example, the progressive loss of the bromide anion resulted in signals corresponding to $[\mathbf{14b}\text{-Br}]^+$ (*m/z* 1341), $[\mathbf{14b}\text{-2Br}]^{2+}$ (*m/z* 631) and $[\mathbf{14b}\text{-3Br}]^{3+}$ (*m/z* 394). Signals resulting from the deprotonation and subsequent loss of HBr such as $[\mathbf{14b}\text{-2HBr} + \text{H}]^+$ (*m/z* 1261), $[\mathbf{14b}\text{-3HBr} + \text{H}]^+$ (*m/z* 1181), $[\mathbf{14b}\text{-4HBr} + \text{H}]^+$ (*m/z* 1101), $[\mathbf{14b}\text{-3HBr} + 2\text{H}]^{2+}$ (*m/z* 591) and $[\mathbf{14b}\text{-4HBr} + 2\text{H}]^{2+}$ (*m/z* 551) were also observed (Figure 2). The isotope patterns obtained by experiment agree with those simulated on the basis of natural abundances.

An increase in sample cone voltage results in intense gas phase fragmentations with signals appearing at repetitive distances corresponding to the loss of an amine moiety (Figure 2). Intramolecular hydrogen bonding between one of the OH groups on a resorcinol ring and the amine nitrogen supports the 1,4-elimination proceeding through a six-membered transition state structure (Scheme 2). All four arms of the tetrabenzoxazines were successfully fragmented at higher voltages. A similar pattern was observed for all *N*-alkylammonium resorcinarene halide cavitands in the gas phase (see Figures S1–S3 of the Supporting Information, available online).

Single crystal X-ray crystallographic studies

The charge-neutral *N*-alkylammonium resorcinarene halides **11–17**, with their flower-like shape and a cavity of suitable size for accepting the small guests, present an interesting family of compounds for inclusion studies. The recrystallisation studies from several solvents or solvent mixtures resulted in altogether seven new single crystal X-ray structures. Table 2 (see Experimental

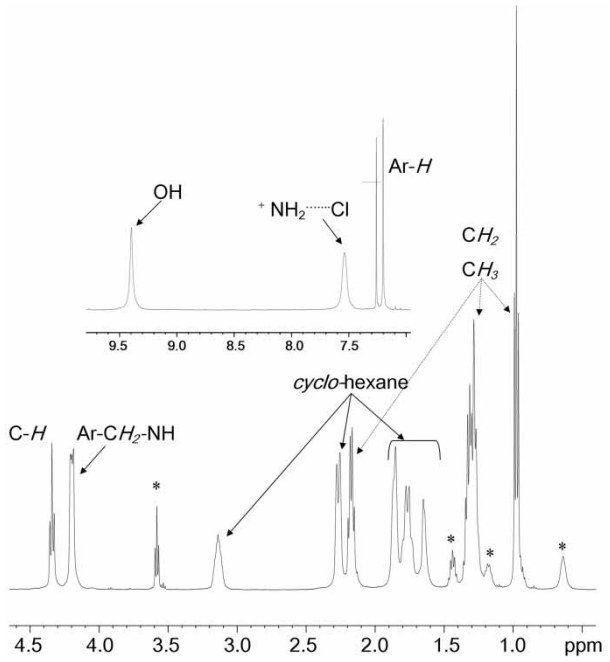

Figure 1. ^{1}H NMR spectrum of **14a** in $CDCl_3$ at 303 K, revealing a triplet for the CH of the resorcinarene skeleton and a broad signal for the diastereotopic $ArCH_2N$. The inset shows the different signals corresponding to OH and NH_2^+ protons. The asterisk corresponds to *n*-butanol from the synthesis.

section) summarises the crystal data of these complexes. Depending on the nature and length of the upper rim chain (R′, Scheme 1) and size of the solvent or guest molecule(s) used for recrystallisation studies, two different types of complexes are formed, self-included or host–guest complexes. In **13b** (sesquihydrate), one of the upper rim propyl chains perfectly fits in the cavity of another molecule, so forming self-included dimer (Figure 3(a)) via N—H···Br hydrogen bond (see Table S1 of the Supporting Information, available online).

The dimer consists of two self-included resorcinarene tetracations and six bromide anions. Four of the bromides are hydrogen bonded between six positively charged nitrogen atoms, and two self-included propylammonium chains share the remaining two bromides, each of which being H-bonded to four ammonium cations (Scheme 3).

The remaining two bromide anions are located outside, linking the dimers via intermolecular hydrogen bonds (see Table S1 of the Supporting Information, available online). The nitrogen atoms in **13b** form an almost perfect square, with the N···N distance difference of 0.04 Å (Table 1; Figure 3(b)). The resorcinarene core in **13b** is nearly symmetrical with distances between the opposite phenyl ring centroids being 6.84 and 6.86 Å (Table 1). The

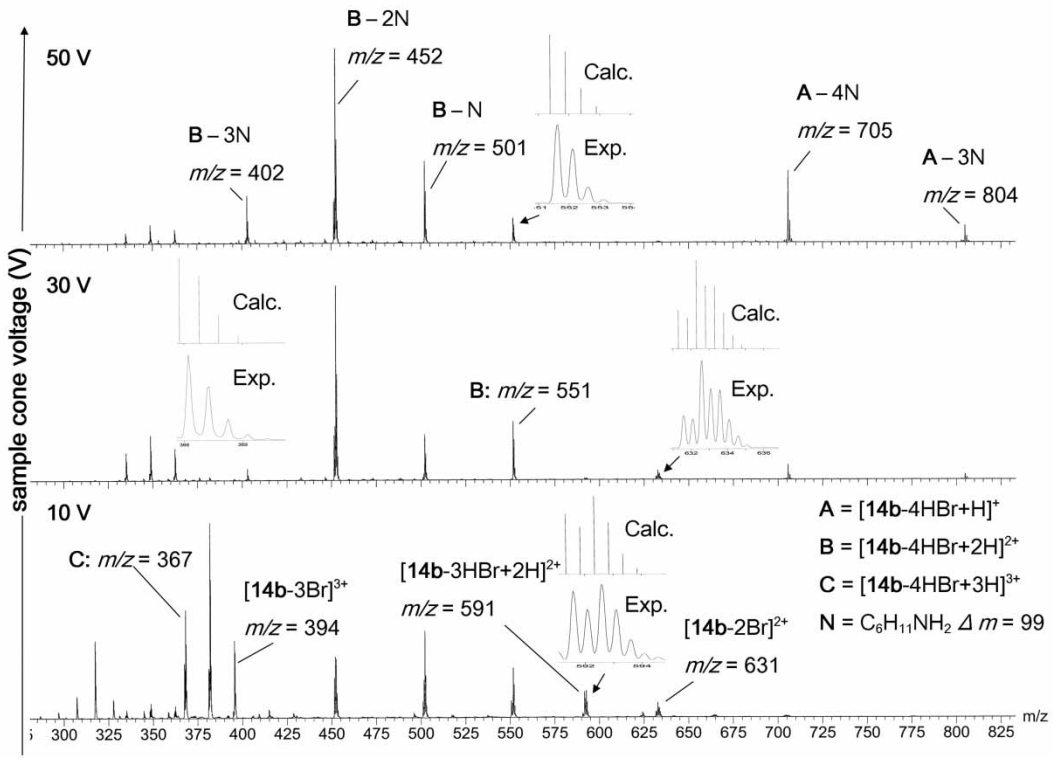

Figure 2. ESI mass spectra of **14b** at different sample cone voltages showing from singly to triply charged species with systematic fragmentation pattern resulting from the loss of amine moieties.

Downloaded At: 14:39 29 January 2011

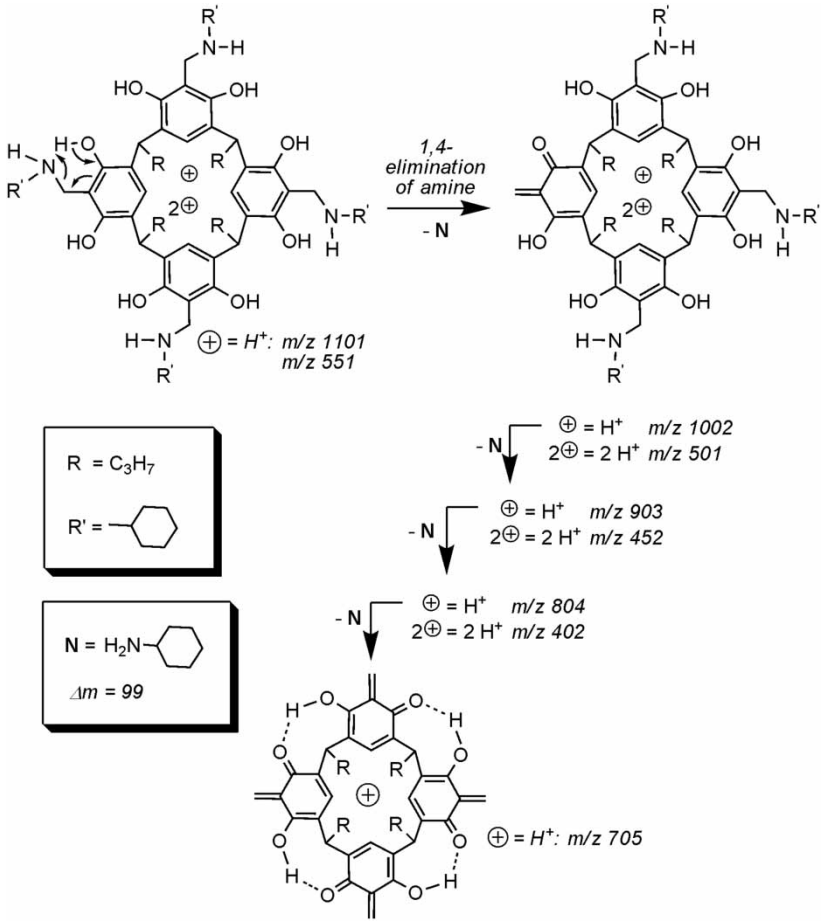

Scheme 2. Fragmentation mechanism and pathways for the consecutive 1,4-eliminations of the amine from protonated **14**.

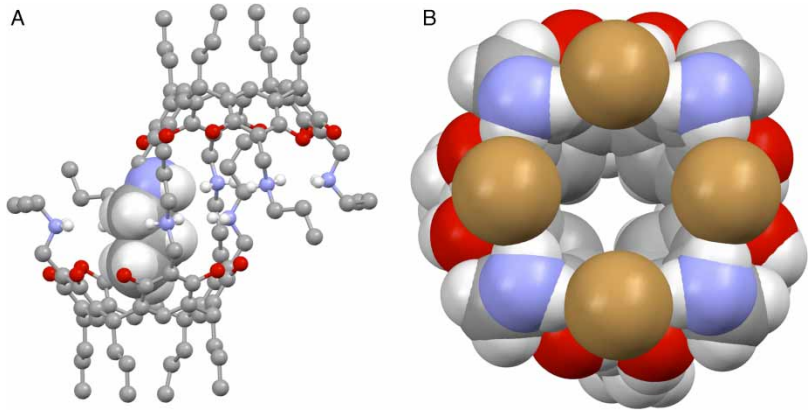

Figure 3. (a) Ball and stick representation of the self-inclusion complex of **13b**. Atoms of one self-included propyl chain as well as nitrogen atom to which they are attached are presented in CPK style. The bromide anions and hydrogen atoms bonded to carbon atoms have been omitted for clarity. (b) CPK plot of **13b** (from the top), showing an almost perfect square formed by four bromide anions and four ammonium cations at the upper rim of the resorcinarene core. The upper rim propyl chains have been omitted for clarity.

minimum distance between the methyl group C39 (denoted as C_T) of the included propyl chain and the centroid (denoted as C_g) of one of four resorcinarene phenyl rings of 3.43 Å is slightly longer than the sum of the van der Waals radii of methyl and phenyl carbon atoms (Table 1). The methyl group is not situated in the centre of the cavity, and the C38—C39 bond is directed towards one phenyl (C15—C20) ring, enabling C—H$\cdots\pi$ interaction [H39A$\cdots C_g$ = 2.93 Å]. Due to steric reasons, one of the non-included propyl chains (C43—C45) at upper rim has

Downloaded At: 14:39 29 January 2011

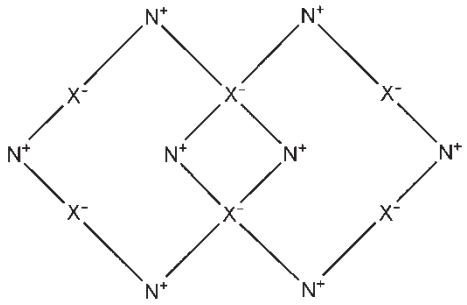

Scheme 3. Schematic representation of the orientation of the positively charged nitrogen atoms and halide anions in the self-included dimers.

to adopt a different orientation and points away from the dimer (Figure 3(a)).

The chloride **13a** crystallises in two slightly different forms, a monohydrate (designated as **13aW**) with almost similar unit cell parameters as **13b** (sesquihydrate) (Table 2, see Experimental section) and butanol solvate hemihydrate (**13aB**). As expected, the replacement of the bromide anions with chlorides results in slightly shorter N···N and $X^-\cdots X^-$ distances in **13aW**, and the cavity at the upper rim is therefore slightly more closed than that in **13b** (Table 1). The chloride anions and ammonium cations form again an almost perfect square (Figure 4(a)). The methyl group of the propyl group is even closer to one of the phenyl rings (Table 1; Figure 4(b)) than in **13b**. Hence, self-inclusion formed by two N—H···Cl hydrogen bonds (see Table S2 of the Supporting Information, available online) is accompanied by two C—H···π interactions, in which hydrogens of the C39 atom point to the C8—C13 and C15—C20 rings, respectively [H39A···C_g (C8—C13) = 2.92 Å; H39C···C_g (C15—C20) = 2.89 Å].

In **13aB**, the butanol solvate hemihydrate of **13a**, the butanol molecule participates in linking self-included dimers via hydrogen bonds (see Table S3 of the Supporting Information, available online). Even though the only difference between **13aW** and **13aB** are the solvent molecules, the included propyl chains in **13aB** is so far from the chloride anion that one hydrogen atom of ammonium nitrogen N30 does not participate in the formation of N—H···Cl hydrogen bonding rings inside resorcinarene core and points to the chloride which is outside of the dimer (Figure 5(a)). This is a consequence of completely different conformation of the self-included propyl group. The propyl group is not directed towards the bottom of the cavity as in **13aW**, in which the propyl group adopts an almost perfect antiperiplanar conformation defined by the propyl chain torsion angles C5—C29—N30—C37, C29—N30—C37—C38 and N30—C37—C38—C39 of −179.0(6)°, −178.5(6)° and 179.5(6)°, respectively. The propyl chain inside the cavity in **13aB** is twisted, the C5—C29—N30—C37 and N30—C37—C38—C39 torsion angles being 83.1(5)° and −71.6(6)°, respectively (Figure 5(b)). Consequently, the C39···C_g (C15—C20) distance is 0.12 Å longer than in **13aW** (Table 1), and such orientation of the propyl group prevents C—H···π interaction formation. Furthermore, the upper rim defined by N···N distances is more opened than in **13aW** resulting in much bigger cavity for self-inclusion (Figure 5(a)). Lower rim is also more distorted than in **13b** and **13aW**, so that resorcinarene core in **13aB** adopts distorted conformation (Table 1).

The C_2 analogue of the bromide **13b**, viz. **11b** (Figure 6) was recrystallised from the mixture of acetonitrile, dichloromethane and butanol as a hemihydrate. The upper rim of the resorcinarene core is only slightly distorted with the difference between opposite N···N distances of 0.16 Å, while the distance between phenyl ring centroids differs for only 0.05 Å (Table 1). Such conformation of the resorcinarene core in **11b** corresponds to that of previously published

Table 1. Geometrical parameters defining conformation of the resorcinarene core and interaction distances.

	11a	**11b**	**12b**	**13aW**	**13aB**	**13b**	**17a**
Core conformation							
$C_g\cdots C_g$ distance (Å)							
C1—C6/C15—C20	6.47, 6.51	6.83	7.20	6.83	6.92	6.84	6.96
C8—C13/C22—C27	7.13, 7.10	6.88	6.40	6.84	6.80	6.86	6.77
N···N distance (Å)							
N30···N34	7.63, 8.07	8.84	10.00	8.67	9.47	8.90	9.79
N32···N36	9.22, 9.04	9.00	7.86	8.62	8.99	8.94	8.54
$X^-\cdots X^-$ distance (Å)							
X1···X3	8.24, 8.09	7.47	8.28	7.20	7.39	7.41	8.80
X2···X4	7.43, 7.55	7.81	7.73	7.60	7.65	7.81	8.50
Inclusion							
$C_T\cdots C_g$ distance (Å)	$C_T = C_{DCM}$	$C_T = C_{Pr}$	$C_T = C_{MeOH}$	$C_T = C_{Pr}$	$C_T = C_{Pr}$	$C_T = C_{Pr}$	$C_T = C_{BuOH}$
$C_T\cdots C_g$(C1—C6)	3.54, 3.90	3.71	4.59	4.02	4.24	4.06	4.29
$C_T\cdots C_g$(C8—C13)	3.86, 3.58	4.08	3.93	3.71	3.94	3.80	3.94
$C_T\cdots C_g$(C15—C20)	3.56, 3.90	3.79	3.93	3.41	3.53	3.43	3.57
$C_T\cdots C_g$(C22—C27)	3.99, 3.58	3.45	3.70	3.74	3.77	3.73	3.71

Downloaded At: 14:39 29 January 2011

Downloaded At: 14:39 29 January 2011

Table 2. X-ray crystallographic data for **11a**, **11b**, **12b**, **13aW**, **13aB**, **13b** and **17a**.

	11a	**11b**	**12b**	**13aW**	**13aB**	**13b**	**17a**
Empirical formula	$(C_{52}H_{80}Cl_4N_4O_8{\cdot}2CH_2Cl_2)_2$	$C_{52}H_{80}Br_4N_4O_8{\cdot}0.5H_2O$	$C_{64}H_{96}Br_4N_4O_8{\cdot}CH_3OH$	$C_{56}H_{88}Cl_4N_4O_8{\cdot}H_2O$	$C_{56}H_{88}Cl_4N_4O_8$ $C_4H_9OH{\cdot}0.5H_2O$	$C_{56}H_{88}Br_4N_4O_8{\cdot}1.5H_2O$	$C_{76}H_{120}Cl_4N_4O_8{\cdot}C_4H_9OH{\cdot}CHCl_3$
Formula weight	1801.28	1217.85	1401.13	1105.12	1170.23	1286.96	1553.05
Crystal system	Monoclinic	Triclinic	Orthorhombic	Triclinic	Triclinic	Triclinic	Triclinic
Space group	*P*2/*n*	$P\bar{1}$	*Pbca*	$P\bar{1}$	$P\bar{1}$	$P\bar{1}$	$P\bar{1}$
Unit cell dimensions							
a (Å)	22.5428(7)	14.088(6)	22.9927(4)	15.0305(16)	15.6728(6)	14.9763(7)	12.9757(2)
b (Å)	11.7229(5)	15.988(5)	23.6470(3)	15.6904(15)	15.6801(6)	15.9466(4)	16.8203(2)
c (Å)	34.7978(13)	16.198(8)	25.6885(4)	15.8794(14)	16.1096(5)	16.1489(5)	22.0248(4)
α (°)	90	61.01(3)	90	119.461(7)	102.931(2)	119.455(2)	107.2380(10)
β (°)	102.590(2)	71.70(5)	90	96.716(6)	110.825(2)	97.571(2)	93.5560(10)
γ (°)	90	77.71(2)	90	98.353(4)	99.3890(10)	98.571(2)	111.5530(10)
V (Å^3)	8974.8(6)	3022(2)	13967.1(4)	3148.0(5)	3476.1(2)	3225.1(2)	4190.32(11)
Z	4	2	8	2	2	2	2
D_{calc} (g cm^{-3})	1.333	1.338	1.333	1.166	1.118	1.325	1.231
Absorption coeff. μ (mm^{-1})	0.430	3.654	2.359	0.240	0.222	2.547	0.293
θ range (°)	1.20–25.00	3.92–63.48	1.47–25.00	1.53–25.00	1.71–25.00	2.29–25.00	3.06–25.00
Collected reflections no.	41,214	29,352	103,167	22,930	25,143	22,752	42,656
Independent refl. no. (R_{Int})	15601/0.0743	9563/0.1187	12306/0.1034	11032/0.0733	12163/0.0518	11055/0.0637	14682/0.0673
Reflections no. $I \geq 2\sigma(I)$	9709	6105	7463	4910	6926	6725	8037
Data/restraints/parameters	15601/48/1068	9563/40/657	12306/0/753	11032/24/674	12163/3/721	11055/21/669	14682/75/932
Goodness-of-fit on F^2, *S*	0.976	0.925	0.986	0.998	0.986	0.940	0.887
R $[I \geq 2\sigma(I)]$/*R* [all data]	0.0753/0.1349	0.0918/0.1274	0.0730/0.1297	0.1118/0.2082	0.0894/0.1463	0.0827/0.1348	0.1035/0.1735
wR $[I \geq 2\sigma(I)]$/*wR* [all data]	0.2262/0.2822	0.2442/0.2748	0.1729/0.1950	0.2775/0.3215	0.2528/0.2856	0.2031/0.2298	0.2736/0.3114
Max/min. el. dens. (e Å^{-3})	1.094/−1.189	1.961/−1.251	1.423/−0.731	1.199/−0.462	2.490/−1.119	1.665/−1.541	1.277/−1.205

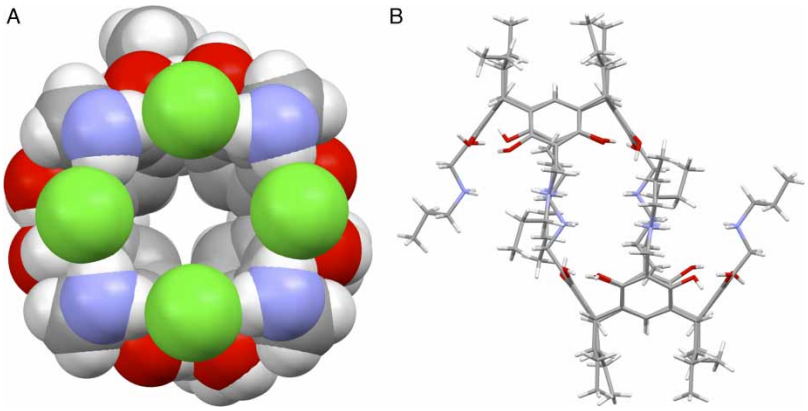

Figure 4. (a) CPK plot of **13aW** (from the top), showing an almost perfect square formed by four chlorides and four ammonium moieties of the upper rim of the resorcinarene core. The upper rim propyl chains have been omitted for clarity. (b) Capped sticks representation of self-inclusion of **13aW** showing position of the self-included propyl groups. Chlorides and lattice water have been omitted for clarity.

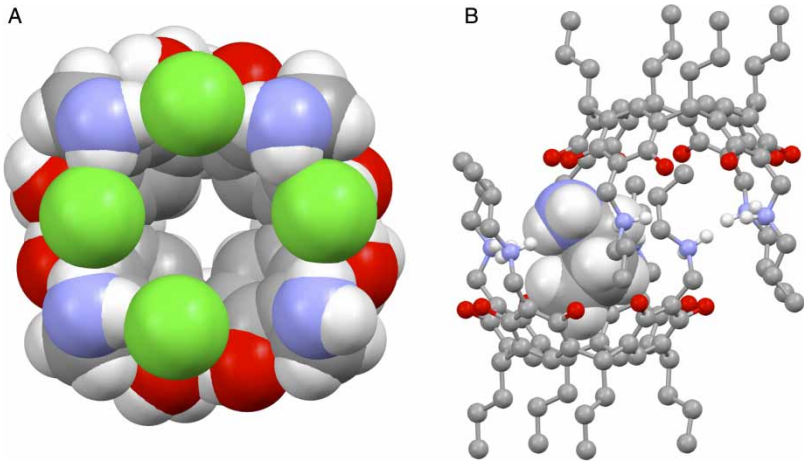

Figure 5. (a) CPK plot of **13aB** (from the top), showing the spatial deformation of the ammonium moieties and chloride anions. The upper rim propyl chains have been omitted for clarity. (b) Ball and stick representation of self-inclusion in **13aB**, showing self-included propyl chain in CPK style. Chloride anions and hydrogen atoms bonded to carbon atoms and solvent molecules are omitted for clarity.

Downloaded At: 14:39 29 January 2011

(*11a*) *n*-butylammonium chloride analogue of structures presented here (*11a*) (R′ = *n*-butyl, R = methyl; Scheme 1). As in **13b** and **13aW**, the self-included dimers are joined via two of the six bromides by H-bonds to the ammonium centres, while remaining two disordered bromides link the dimers via hydrogen bonds (see Table S4 of the Supporting Information, available online). The orientation of the self-included propyl group inside the cavity is enabled via two C—H···π interactions, pointing towards the phenyl rings (C22—C27 and C1—C6) with almost identical geometry [H···C_g(C22—C27) = 2.88 Å, C—H···C_g = 118°; H···C_g(C1—C6) = 2.93 Å, C—H···C_g = 137°].

For recrystallisation studies of the chloride analogue **11a**, butanol was not used and the usage of acetonitrile and dichloromethane mixture resulted in an unexpected disruption of the self-included dimer, and instead inclusion of dichloromethane molecules into the cavity was observed. The **11a** crystallises with $Z' = 2$, and dichloromethane molecules fill up the cavities of both independent resorcinarene molecules with the host:guest ratio of 1:2 (Figure 7(a)). Unlike in all previous halides, now the four chloride anions are H-bonded between the ammonium moieties of the resorcinarene (see Table S5 of the Supporting Information, available online). The inclusion of the dichloromethane molecules results in a highly distorted resorcinarene conformation as a consequence of repulsion between dichloromethane chlorines and atoms of the anion–cation belt (Table 1; Figure 7(b)). Distortion is strongly pronounced even in the resorcinarene core with the C_g···C_g distance differences of 0.66 and 0.59 Å. Thus, the geometry of the resorcinarene core is markedly influenced by the inclusion of dichloromethane molecules. The dichloromethane molecules (DCM) sit on top of each other inside the cavity, the lower dichloromethane molecule is situated at the bottom of the cavity, while the second one is placed slightly above the cation–anion belt at the upper

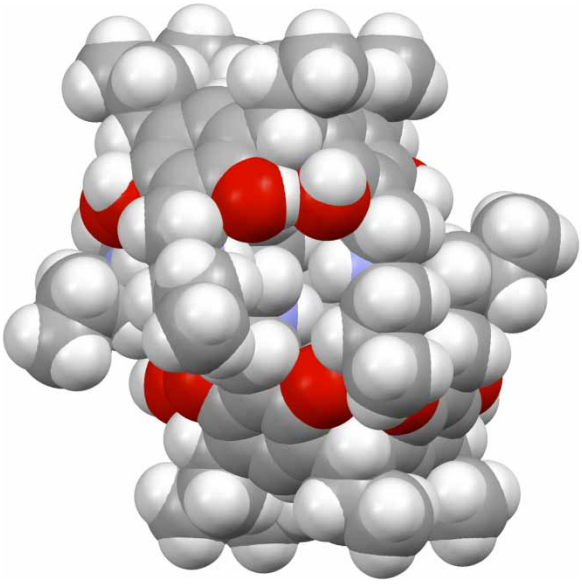

Figure 6. CPK plot of the dimer of **11b**. Bromide anions have been omitted for clarity. For clarity, only one component of disordered atom C54 is shown.

Downloaded At: 14:39 29 January 2011

rim (Figure 7(a)). The shortest $C_T(DCM)\cdots C_g$ distances for dichloromethane molecules at lower position in both cavities are approximately the same, so indicating their similar position inside the cavity. The chlorine atoms of the dichloromethane molecules within the same cavity are rotated and displaced in staggered orientation in order to minimise their repulsion (Figure 7(a),(b)), yet the orientation of the dichloromethane is different in both resorcinarenes. Each dichloromethane carbon atom on lower position participates with both hydrogen atoms in two C—H$\cdots\pi$ interactions with $H\cdots C_g$ distances which are shorter compared to **11b** [H1A$\cdots C_g$(C1A—C6A) = 2.68 Å; H1B$\cdots C_g$(C15A—C20A) = 2.72 Å; H3A$\cdots C_g$(C8B—C13B) = 2.78 Å].

In the cyclohexyl analogue of **11b** and **13b**, viz. **12b**, the self-inclusion and subsequent dimer formation is not possible due to the sterically very bulky cyclohexyl groups. When methanol is used as the recrystallisation solvent, only simple methanol inclusion complex is formed (Figure 8). As a consequence of the larger sterical demand of the cyclohexyl groups and the bromide anions, the cation–anion belt is more distorted than in other bromides (**11b** and **13b**), even the overall conformation of the resorcinarene core is affected (Table 1). The difference in distance between opposite ring centroids and opposite N$\cdots$N atoms is 0.80 and 2.14 Å, respectively.

Each cyclohexyl group has a slightly different orientation towards the resorcinarene core and the groups are disposed in propeller-like fashion (Figure 8). The included methanol molecule sits on the upper part of the cavity, slightly below the plane of the cation–anion belt, and in a position which enables O—H$\cdots$Br hydrogen bond formation (see Table S6 of the Supporting Information, available online). Therefore, it is closer to the bromide to which it generates hydrogen bond. The carbon atom of the methanol molecule is too far away from the phenyl rings, and therefore, no C—H$\cdots\pi$ interactions are observed.

In our preliminary work (*11a*), we have shown that *N*-alkylammonium resorcinarene halide cavitands bind short-chained aliphatic alcohols, showing the selectivity towards *n*-butanol. The C_5 analogue of **12a**, viz. **17a**, represents such an example in which the *N*-alkylammonium resorcinarene chloride acts as a size-selective receptor for *n*-butanol. In addition to the deeply included *n*-butanol, one molecule of chloroform sits on top of the cation–anion belt just as in the dichloromethane-included **11a**. The *n*-butanol is deeply buried inside the cavity, and similarly as the methanol molecule in **12b**, the OH group of the *n*-butanol is situated on the cation–anion belt between the chloride anion and the ammonium moiety with a $Cl^-\cdots H—O\cdots H—N^+$ hydrogen bond motif (Figure 9(a),(b); see Table S7 of the Supporting Information, available online). As in other host–guest complexes, the resorcinarene core adopts a distorted conformation. There is also one C—H$\cdots\pi$ interaction

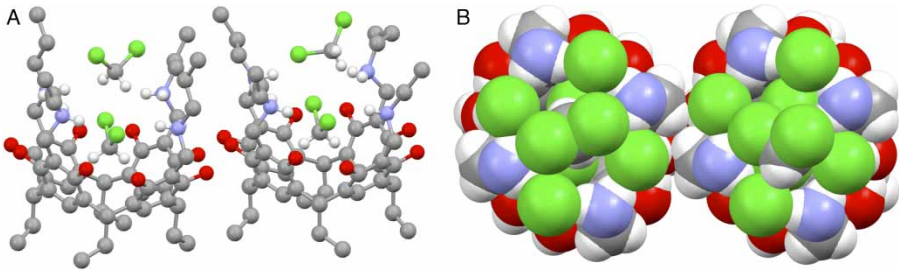

Figure 7. (a) Ball and stick representation of **11a**, showing position of the dichloromethane molecules in the cavity of the two independent complexes. The chloride anions and hydrogen atoms bonded to carbon atoms of the cations have been omitted for clarity. (b) CPK plots of two **11a**·$2CH_2Cl_2$ complexes showing the distorted conformation of the upper rim cation–anion belt and staggered orientation of dichloromethane molecules. Upper rim propyl chains have been omitted for clarity. For clarity, only major component of the disordered atoms C41A, C42A, C52A, C56A and C4 is shown.

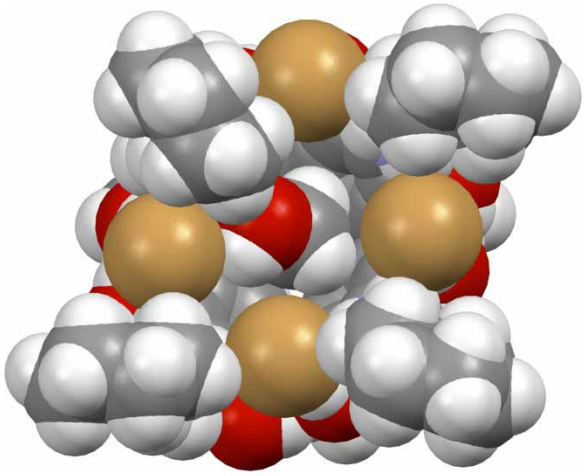

Figure 8. CPK plot of **12b** showing the included methanol molecule, which is hydrogen bonded to one of the bromide anions.

between the hydrogen of the butanol molecule methyl group and phenyl ring [H81A···C_g(C22–C27) = 2.90 Å].

Conclusion

The synthesis and structural studies of several hydrogen bond-stabilised *N*-alkylammonium resorcinarene chloride and bromide cavitands are reported. These compounds are symmetrical in solution by NMR spectroscopy and show typical fragmentation pattern in the gas phase by tuning the sample cone voltage. X-ray crystal structural study of seven of these cavitands revealed that when the upper rim ammonium moiety is functionalised with a short alkyl chain, viz. a propyl chain, complementary self-inclusion dimers are formed (**11b**, **13aW**, **13aB** and **13b**) in all except one case (**11a**). In the case of **11a** or with cyclohexylammonium halides, host–guest complexes with the solvent molecule inclusion are obtained. In all of the self-included dimer complexes, the dimer consists of extensively hydrogen-bonded *N*-alkylammonium resorcinarene tetracations and six halide anions, the remaining two halide anions link the dimers via H-bonds. In dimer complexes, the resorcinarene core has nearly symmetrical cone conformation due to the complementary structures of the dimer halves. The conformation of the host–guest inclusion complexes is much more influenced by the size, shape and guest to host H-bonding than in the dimers. Both protic and aprotic guest molecules are included into the resorcinarene cavity. As the cavity is much more extended than in regular resorcinarenes, a simultaneous inclusion of two molecules is observed as 1:2 complexes, the first guest deep in the cavity and the second on top of the first one; two dichloromethane molecules in **11a** and butanol and chloroform molecules in **17a**. In both cases, the second included guest molecule was non-polar, and thus in the case of polar protic methanol, only the 1:1 inclusion complex (**12b**) was formed. The protic-included molecules, methanol and butanol, were hydrogen bonded to the halide, in the case of longer butanol, $Cl^{-}\cdots H{-}O\cdots H{-}N^{+}$ hydrogen bond motif is observed. The deep cavity and the cation–anion belt of the cavitands **11**–**17** offer possibilities to create size-selective receptors for suitably sized molecules with H-bond donor sites such as alcohols, amides and ammonium ions, and this work is currently in progress in our laboratory.

Experimental

General remarks

Melting points were determined with a Mettler Toledo FP62 capillary melting point apparatus and are uncorrected. Elemental analyses were carried out with a Varian ELIII elemental analyser. ^{1}H and ^{13}C NMR spectra were recorded on Bruker Avance DRX 500 (500 MHz for ^{1}H

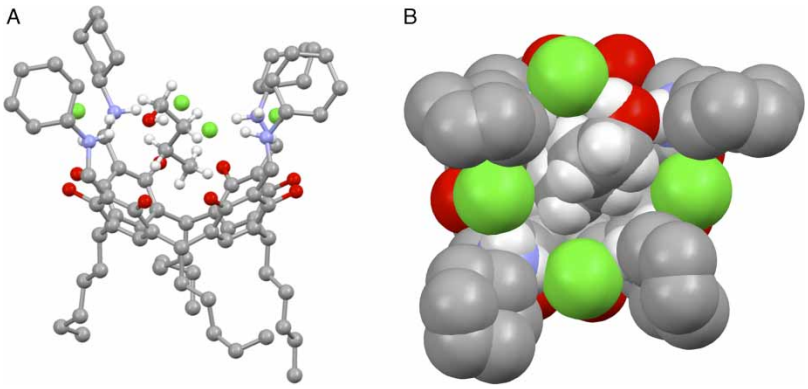

Figure 9. (a) Ball and stick representation of **17a** showing position of the *n*-butanol molecule in the cavity. The chloroform molecule and the hydrogen atoms of the carbons of the cation have been omitted for clarity; (b) CPK plot of **17a** (from the top), showing hydrogen-bonded *n*-butanol and differently orientated cyclohexane rings. Pentyl group atoms, chloroform molecule and the cyclohexyl hydrogens have been omitted for clarity. Only one component of disordered C82 and C83 atoms in both figures is shown.

Downloaded At: 14:39 29 January 2011

and 126 MHz for ^{13}C) or Bruker Avance DRX 250 (250 MHz for ^{1}H and 63 MHz for ^{13}C) spectrometers. The mass spectrometric studies were performed with a micromass LCT ESI-TOF instrument. Since the instrument does not permit MS/MS experiments, the fragmentation behaviour of the samples was examined by in-source fragmentation-induced collisions with the gas molecules present in the ion source. For this purpose, the ions were accelerated to different kinetic energies by tuning the sample cone voltage to different settings. At low voltage, the ions are not significantly accelerated and undergo fragmentations only to a minor extent upon collision with the surrounding gas molecules. With a high sample cone voltage, the ions approach the sample cone at a higher velocity, and collisions with the surrounding gas lead to more pronounced fragmentations.

All materials were commercial and used as such unless otherwise mentioned. Compounds **1**–**3**, **5**, **10**, **12a**,**b** and **17a** were synthesised according to reported procedures (*1*,*10*,*11*).

Downloaded At: 14:39 29 January 2011

Synthesis

General procedure for the preparation of the tetrabenzoxazines

Into a solution of resorcinarene and excess formaldehyde in ethanol, 4 equiv. of the amine was slowly added. The mixture was stirred at room temperature for 24 h. The precipitated product was filtered off, washed with cold ethanol/water (9:1 v/v) and dried.

4

Formaldehyde (5 ml), ethanol (90 ml), resorcinarene **1** (4.0 g, 6.7 mmol) and *n*-propylamine (2.7 ml, 33.0 mmol). Yield 2.84 g, 45%. Mp > 300°C (found C, 71.11; H, 8.43; N, 5.72. $C_{56}H_{76}N_4O_8{\cdot}1.0CH_3CH_2OH$ requires C, 71.14; H, 8.43; N, 5.72) [$C_{56}H_{76}N_4O_8$ MW 933.20; ESI-TOF MS $[M + H]^+$933.61]. ^{1}H NMR (250 MHz, $CDCl_3$, 30°C) δ: 7.78 (s, 4H, Ar-O*H*), 7.11 (s, 4H, Ar-H), 4.91 (m, 8H, N-CH_2-O), 4.13 (t, $J = 7.6$ Hz, 4H, C*H*), 3.93 (d, $J = 17.3$ Hz, 4H, Ar-CH_2-N), 3.75 (d, $J = 17.3$ Hz, 4H, Ar-CH_2-N), 2.59 (m, 8H, CH_2), 2.18 (m, 8H, CH_2), 1.53 (m, 8H, CH_2), 0.89 (m, 24H, CH_3); ^{13}C NMR (63 MHz, $CDCl_3$, 30°C) δ: 149.75, 148.12, 124.09, 123.38, 120.98, 108.57, 83.12, 53.46, 46.31, 34.83, 26.62, 21.18, 12.63, 11.54.

6

Formaldehyde (5 ml), ethanol (90 ml), resorcinarene **2** (3.0 g, 4.6 mmol) and *n*-propylamine (1.5 ml, 18.0 mmol). Yield 3.23 g, 71%. Mp > 300°C (found C, 71.39; H, 8.38; N, 5.11. $C_{60}H_{84}N_4O_8{\cdot}1.0CH_3CH_2OH{\cdot}0.5H_2O$ requires C, 71.30; H, 8.78; N, 5.36) [$C_{60}H_{84}N_4O_8$ MW 989.40; ESI-TOF MS $[M + H]^+$989.66]. ^{1}H NMR (250 MHz, $CDCl_3$, 30°C) δ: 7.77 (s, 4H, Ar-O*H*), 7.12 (s, 4H, Ar-*H*), 4.91 (m, 8H, N-CH_2-O), 4.25 (t, $J = 7.8$ Hz, 4H, C*H*), 3.92 (d, $J = 17.3$ Hz, 4H, Ar-CH_2-N), 3.74 (d, $J = 17.5$ Hz, 4H, Ar-CH_2-N), 2.58 (m, 8H, CH_2), 2.17 (m, 8H, CH_2), 1.52 (m, 8H, CH_2), 1.31 (m, 8H, CH_2), 0.98 (t, $J = 7.3$ Hz, 12H, CH_3), 0.88 (t, $J = 7.3$ Hz, 12H, CH_3); ^{13}C NMR (63 MHz, $CDCl_3$, 30°C) δ: 149.66, 148.02, 124.21, 123.41, 121.14, 108.54, 83.12, 53.43, 46.29, 35.59, 32.30, 21.17, 21.08, 13.96, 11.53.

7

Formaldehyde (3 ml), ethanol (30 ml), resorcinarene **2** (1.0 g, 1.5 mmol) and cyclohexylamine (0.70 ml, 6.1 mmol). Yield 1.40 g, 80%. Mp = 268°C (found C, 73.65; H, 8.54; N, 4.42. $C_{72}H_{100}N_4O_8{\cdot}0.75CH_3CH_2OH$ $0.5H_2O$ requires C, 73.99; H, 8.91; N, 4.70) [$C_{72}H_{100}N_4O_8$ MW 1149.60; ESI-TOF MS $[M + H]^+$1149.90]. ^{1}H NMR (250 MHz, $CDCl_3$, 30°C) δ: 7.72 (s, 4H, Ar-O*H*), 7.13 (s, 4H, Ar-*H*), 5.06 (d, $J = 10.0$ Hz, 4H, N-CH_2-O), 4.98 (d, $J = 10.3$ Hz, 4H, N-CH_2-O), 4.24 (t, $J = 7.8$ Hz, 4H, C*H*), 3.99 (d, $J = 17.5$ Hz, Ar-CH_2-N), 3.89 (d, $J = 17.3$ Hz, 4H, Ar-CH_2-N), 2.59 (m, 8H, CH_2), 2.57 (br s, 4H, C*H*), 1.5–2.3 (m, H, CH_2), 1.1–1.4 (m, H, CH_2), 0.98 (t, $J = 7.3$ Hz, 12H, CH_3); ^{13}C NMR (63 MHz, 30°C, DMSO-d_6) δ: 149.25, 148.95, 124.15, 123.52, 121.02, 109.57, 80.60, 57.98, 43.66, 35.68, 32.21, 31.89, 31.15, 30.85, 25.88, 25.45, 25.18, 21.07, 13.93.

8

Formaldehyde (3 ml), ethanol (30 ml), resorcinarene **2** (1.0 g, 1.5 mmol) and *n*-hexylamine (0.81 ml, 6.1 mmol). Yield 1.18 g, 67%. Mp > 300°C (found C, 73.06; H, 9.05; N, 4.34. $C_{72}H_{108}N_4O_8{\cdot}0.5CH_3CH_2OH.1.0H_2O$ requires C, 73.14; H, 9.50; N, 4.67) [$C_{72}H_{108}N_4O_8$ MW 1157.70; ESI-TOF MS $[M + H]^+$1158.00]. ^{1}H NMR (250 MHz, $CDCl_3$, 30°C) δ: ^{1}H NMR (250 MHz, 30°C, $CDCl_3$) δ: 7.77 (s, 4H, Ar-O*H*), 7.11 (s, 4H, Ar-*H*), 4.90 (m, 8H, N-CH_2-O), 4.24 (t, $J = 7.6$ Hz, 4H, C*H*), 3.92 (d, $J = 17.3$ Hz, 4H, Ar-CH_2-N), 3.72 (d, $J = 17.5$ Hz, 4H, Ar-CH_2-N), 2.59 (m, 8H, CH_2), 2.17 (m, 8H, CH_2), 1.50 (m, 8H, CH_2), 0.97 (t, $J = 7.3$ Hz, 12H, CH_3), 0.86 (m, 12H, CH_3); ^{13}C NMR (63 MHz, 30°C, $CDCl_3$) δ: 149.67, 148.03, 124.23, 123.42, 121.13, 108.56, 83.04, 51.56, 46.39, 35.60, 32.30, 31.71, 27.98, 26.84, 22.61, 21.08, 14.02, 13.97.

9

Formaldehyde (5 ml), ethanol (50 ml), resorcinarene **2** (1.0 g, 1.5 mmol) and benzylamine (1.3 ml, 12.1 mmol). Yield 1.66 g, 93%. Mp > 300°C (found C, 76.19; H, 6.96; N, 4.10. $C_{76}H_{84}O_8N_4{\cdot}0.5H_2O.0.75CH_3CH_2OH$ requires C, 76.26; H, 7.35; N, 4.59) [$C_{76}H_{84}O_8N_4$ MW 1181.51; ESI-

TOF MS $[M + H]^+$1181.78]. ^{1}H NMR (250 MHz, $CDCl_3$, 30°C) δ: ^{1}H NMR (250 MHz, 30°C, $CDCl_3$) δ: 7.71 (s, 4H, Ar-OH), 7.20–7.29 (m, 24H, Ar-H, Ph-H), 4.88 (dd, $J_{HH} = 9.8$ Hz, $J_{HH} = 9.8$ Hz, 8H, NCH_2O), 4.29 (t, $J_{HH} = 7.9$ Hz, 4H, CH), 3.73–4.09 (m, 16H, NCH_2Ph, NCH_2Ar), 1.37 (m, 8H, CH_2), 2.22 (m, 8H, CH_2), 1.00 (t, $J_{HH} = 7.3$ Hz, 12H, CH_3); ^{13}C NMR (63 MHz, 30°C, $CDCl_3$) δ: 149.81, 148.09, 137.88, 129.00, 128.80, 128.40, 128.22, 127.34, 127.17, 124.38, 123.60, 121.37, 108.51, 84.92, 55.81, 46.59, 35.76, 21.12, 14.00.

General procedure for the preparation of the N-alkylammonium resorcinarene halide cavitands

Into a solution of the tetrabenzoxazine in butanol, conc. HCl or HBr and H_2O were added. The mixture was refluxed for 4 h. After the water and formaldehyde were removed by azeotropic distillation, the remaining butanol was evaporated. A small amount of ethanol/toluene (1:1 v/v) was added, and the solvents were again evaporated. The crude product was titurated with either acetonitrile or diethylether, filtered off and dried.

Downloaded At: 14:39 29 January 2011

11a

Tetrabenzoxazine **4** (1.2 g, 1.3 mmol), 35 ml BuOH, 10 ml conc. HCl, 8 ml H_2O. Yield 0.99 g, 74%. Mp > 300°C (found C, 51.40; H, 6.98; N, 4.17. $C_{52}H_{80}N_4O_8Cl_4$·2.0-$CHCl_3$·1.0$CH_3CH_2CH_2OH$·1.0H_2O requires C, 51.15; H, 6.96; N, 4.11) [$C_{52}H_{80}N_4O_8Cl_4$ MW 1031.10; ESI-TOF MS $[M\text{-}4Cl\text{-}3H]^+$885.70]. ^{1}H NMR (500 MHz, $CDCl_3$, 30°C) δ: 9.30 (br, 8H, Ar-O*H*), 7.77 (br, 8H, N-*H*), 7.20 (s, 4H, Ar-*H*), 4.22 (m, 12H, C*H* + Ar-CH_2-N), 3.08 (m, 8H, N-CH_2), 2.23 (m, 8H, CH_2), 1.94 (m, 8H, CH_2), 1.25 (m, 12H, CH_3), 0.99 (t, $J = 7.2$ Hz, 12H, CH_3); ^{13}C NMR (126 MHz, 30°C, $CDCl_3$) δ: 150.3, 126.2, 125.1, 108.1, 50.3, 43.6, 34.2, 26.0, 20.1, 12.4, 11.0.

11b

Tetrabenzoxazine **4** (1.05 g, 1.13 mmol), 50 ml BuOH, 4 ml conc. HBr, 4 ml H_2O. Yield 0.91 g, 67%. Mp > 300°C [$C_{52}H_{80}N_4O_8Br_4$ MW 1208.8; ESI-TOF MS $[M\text{-}4Br\text{-}3H]^+$ 885.75, $[M\text{-}3Br\text{-}2H]^+$ 965.79]. ^{1}H NMR (500 MHz, $CDCl_3$, 30°C) δ: 8.92 (br, 8H, Ar-O*H*), 7.46 (br, 8H, N-*H*), 7.22 (s, 4H, Ar-*H*), 4.22 (m, 12H, C*H* + Ar-CH_2-N), 3.13 (m, 8H, N-CH_2), 2.23 (m, 8H, CH_2), 2.02 (m, 8H, CH_2), 1.56 (m, 8H, CH_2), 0.99 (t, $J = 7.3$ Hz, 12H, CH_3), 0.93 (t, $J = 7.1$ Hz, 12H, CH_3); ^{13}C NMR (126 MHz, 30°C, $CDCl_3$) δ: 150.1, 125.9, 125.1, 108.0, 51.0, 43.8, 36.3, 25.7, 19.2, 12.5, 11.1.

13a

Tetrabenzoxazine **6** (1.0 g, 1.0 mmol), 25 ml BuOH, 10 ml conc. HCl, 6 ml H_2O. Yield 0.55 g, 50%. Mp > 300°C (found C, 60.08; H, 8.22; N, 4.49. $C_{56}H_{88}N_4O_8Cl_4$·0.25-$CHCl_3$·0.5$CH_3CH_2CH_2OH$·0.25H_2O requires C, 60.39; H, 8.16; N, 4.84) [$C_{56}H_{88}N_4O_8Cl_4$ MW 1087.1; ESI-TOF MS $[M\text{-}4Cl\text{-}3H]^+$ 941.74]. ^{1}H NMR (500 MHz, $CDCl_3$, 30°C) δ: 9.24 (br, 8H, Ar-O*H*), 7.80 (br, 8H, N-*H*), 7.22 (s, 4H, Ar-*H*), 4.34 (t, $J = 7.7$ Hz, 4H, C*H*), 4.17 (br, 8H, Ar-CH_2-N), 3.07 (br, 8H, N-CH_2), 2.17 (m, 8H, CH_2), 1.92 (br, 8H, CH_2), 1.33 (m, 8H, CH_2), 0.98 (t, $J = 6.8$ Hz, 12H, CH_3), 0.83 (t, $J = 7.2$ Hz, 12H, CH_3); ^{13}C NMR (126 MHz, 30°C, $CDCl_3$) δ: 150.2, 126.3, 125.0, 108.7, 50.8, 43.5, 33.9, 20.9, 19.1, 18.8, 13.9, 11.0.

13b

Tetrabenzoxazine **6** (0.51 g, 0.52 mmol), 25 ml BuOH, 4 ml conc. HCl, 4 ml H_2O. Yield 0.45 g, 69%. Mp > 300°C (found C, 52.92; H, 6.89; N, 3.81. $C_{56}H_{88}$-$N_4O_8Br_4$·0.5$CH_3CH_2CH_2OH$·0.75H_2O requires C, 52.95; H, 7.24; N, 4.26) [$C_{56}H_{88}N_4O_8Br_4$ MW 1264.94; ESI-TOF MS $[M\text{-}4Br\text{-}3H]^+$ 941.77, $[M\text{-}3Br\text{-}2H]^+$1021.56]. ^{1}H NMR (500 MHz, $CDCl_3$, 30°C) δ: 8.91 (br, 8H, Ar-O*H*), 7.46 (br, 8H, N-*H*), 7.23 (s, 4H, Ar-*H*), 4.34 (t, $J = 7.8$ Hz, 4H, C*H*), 4.18 (br, 8H, Ar-CH_2-N), 3.12 (br, 8H, N-CH_2), 2.19 (m, 8H, CH_2), 2.01 (br, 8H, CH_2), 1.33 (m, 8H, CH_2), 0.98 (m, 24H, CH_3); ^{13}C NMR (126 MHz, 30°C, $CDCl_3$) δ: 150.0, 126.0, 125.2, 107.9, 51.0, 43.8, 34.7, 20.9, 19.2, 15.2, 13.8, 11.1.

14a

Tetrabenzoxazine **7** (1.3 g, 1.1 mmol), 30 ml BuOH, 10 ml conc. HCl, 8 ml H_2O. Yield 0.87 g, 62%. Mp = 259°C (found C, 64.15; H, 8.40; N, 3.89. $C_{68}H_{104}N_4O_8Cl_4$·0.5-$CH_3CH_2CH_2OH$·1.5H_2O requires C, 64.11; H, 8.61; N, 4.27) [$C_{68}H_{104}N_4O_8Cl_4$ MW 1247.4; ESI-TOF MS $[M\text{-}4Cl\text{-}3H]^+$1101.89, $[M\text{-}3Cl\text{-}2H]^+$1138.20, $[M\text{-}2Br\text{-}H]^+$1174.22]. ^{1}H NMR (500 MHz, $CDCl_3$, 30°C) δ: 9.38 (br, 8H, Ar-O*H*), 7.54 (br, 8H, N-*H*), 7.19 (s, 4H, Ar-*H*), 4.33 (t, $J = 7.9$ Hz, 4H, C*H*), 4.20 (br, 8H, Ar-CH_2-N), 3.13 (br, 4H, C*H*), 2.27 (d, $J = 11.3$ Hz, 8H, CH_2), 2.17 (q, $J = 7.6$ Hz, 8H, CH_2), 1.85 (br, 8H, CH_2), 1.79 (q, $J = 11.5$ Hz, 8H, CH_2), 1.65 (br, 4H, CH_2), 1.28 (m, 20H, CH_2), 0.97 (t, $J = 7.3$ Hz, 12H, CH_3); encapsulated butanol, 1.43 (br, 2H, CH_2), 1.18 (br, 2H, CH_2), 0.63 (br, 3H, CH_3); ^{13}C NMR (126 MHz, 30°C, $CDCl_3$) δ: 150.2, 126.1, 124.8, 108.6, 59.2, 40.4, 34.7, 34.6, 33.8, 28.6, 24.7, 20.9, 13.9; encapsulated butanol, 24.8, 18.7, 13.4.

14b

Tetrabenzoxazine **7** (0.84 g, 0.73 mmol), 30 ml BuOH, 4 ml conc. HBr, 4 ml H_2O. Yield 0.74 g, 81%. Mp = 266°C (found C, 56.94; H, 7.41; N, 3.43. $C_{68}H_{104}N_4O_8Br_4$·1.0-$CH_3CH_2CH_2OH$·1.0H_2O requires C, 56.99; H, 7.71; N, 3.69) [$C_{68}H_{104}N_4O_8Br_4$ MW 1247.39 ESI-TOF MS [M-

4Br-3H]$^+$11102.24, [M-3Br-2H]$^+$1182.21, [M-2Br-H]$^+$1262.16]. ^{1}H NMR (500 MHz, $CDCl_3$, 30°C) δ: 8.96 (br, 8H, Ar-O*H*), 7.25 (br, 8H, N–*H*), 7.22 (s, 4H, Ar-*H*), 4.34 (t, $J = 7.8$ Hz, 4H, C*H*), 4.19 (br, 8H, Ar-CH_2-N), 3.22 (br, 4H, C*H*), 2.33 (d, $J = 10.5$ Hz, 8H, CH_2), 2.18 (q, $J = 7.6$ Hz, 8H, CH_2), 1.88 (br, 16H, CH_2), 1.65 (br, 4H, CH_2), 1.29 (m, 20H, CH_2), 0.97 (t, $J = 7.3$ Hz, 12H, CH_3); ^{13}C NMR (126 MHz, 30°C, $CDCl_3$) δ: 150.0, 125.9, 125.0, 107.8, 59.7, 40.8, 34.8, 33.7, 28.6, 24.7, 20.9, 13.8.

15a

Tetrabenzoxazine **8** (0.6 g, 0.52 mmol), 15 ml BuOH, 6 ml conc. HCl, 5 ml H_2O. Yield 0.12 g, 18%. Mp > 300°C (found C, 59.81; H, 8.41; N, 3.84. $C_{68}H_{112}N_4O_8Cl_4 \cdot 1.0CHCl_3$ requires C, 60.28; H, 8.28; N, 4.08) [$C_{68}H_{112}N_4O_8Cl_4$ MW 1255.4; ESI-TOF MS [M-4Cl-3H]$^+$1145.89]. ^{1}H NMR (500 MHz, $CDCl_3$, 30°C) δ: 9.31 (br, 8H, Ar-O*H*), 7.72 (br, 8H, N-*H*), 7.21 (s, 4H, Ar-*H*), 4.34 (t, $J = 7.8$ Hz, 4H, C*H*), 4.18 (br, 8H, Ar-CH_2-N), 3.11 (br, 8H, N-CH_2), 2.18 (q, $J = 7.6$ Hz, 8H, CH_2), 1.88 (m, 8H, CH_2), 1.67 (br, 4H, CH_2), 1.33 (m, 28H, CH_2), 0.98 (t, $J = 7.3$ Hz, 12H, CH_3), 0.85 (t, $J = 6.9$ Hz, 12H, CH_3); ^{13}C NMR (126 MHz, 30°C, $CDCl_3$) δ: 150.2, 126.3, 124.9, 108.8, 49.5, 43.7, 34.6, 33.9, 31.0, 26.2, 25.5, 22.3, 21.0, 13.9, 13.8.

15b

Tetrabenzoxazine **8** (0.4 g, 0.34 mmol), 25 ml BuOH, 2 ml conc. HBr, 3 ml H_2O. Yield 0.38 g, 77%. Mp > 300°C (found C, 56.03; H, 7.61; N, 3.39. $C_{68}H_{112}N_4O_8Br_4 \cdot 1.5H_2O \cdot 0.25CH_3CH_2CH_2CH_2OH$ requires C, 56.04; H, 8.01; N, 3.79) [$C_{68}H_{112}N_4O_8Br_4$ MW 1433.25; ESI-TOF MS [M-4Br-3H]$^+$1110.04, [M-3Br-2H]$^+$1191.97]. ^{1}H NMR (500 MHz, $CDCl_3$, 30°C) δ: 8.94 (br, 8H, Ar-O*H*), 7.46 (br, 8H, N-*H*), 7.23 (s, 4H, Ar-*H*), 4.35 (t, $J = 7.9$ Hz, 4H, C*H*), 4.17 (br, 8H, Ar-CH_2-N), 3.15 (br, 8H, N-CH_2), 2.19 (q, $J = 7.5$ Hz, 8H, CH_2), 1.97 (m, 8H, CH_2), 1.57 (br, 4H, CH_2), 1.30 (m, 28H, CH_2), 0.98 (t, $J = 7.3$ Hz, 12H, CH_3), 0.86 (t, $J = 7.0$ Hz, 12H, CH_3); ^{13}C NMR (126 MHz, 30°C, $CDCl_3$) δ: 150.0, 126.0, 125.2, 108.0, 49.6, 43.8, 34.7, 33.8, 31.0, 26.3, 25.4, 22.3, 20.9, 13.9, 13.8.

16a

Tetrabenzoxazine **9** (0.5 g, 0.42 mmol), 15 ml BuOH, 5 ml conc. HCl, 5 ml H_2O. Yield 0.21 g, 39%. Mp > 300°C (found C, 66.37; H, 7.07; N, 4.09. $C_{72}H_{88}N_4O_8Cl_4 \cdot 1.0H_2O$ requires C, 66.66; H, 6.99; N, 4.32) [$C_{72}H_{88}N_4O_8Cl_4$ MW 1279.3; ESI-TOF MS [M-4Cl-3H]$^+$1133.61]. ^{1}H NMR (500 MHz, $CDCl_3$, 30°C) δ: 9.10 (br, 8H, Ar-O*H*), 8.09 (br, 8H, N-*H*), 7.68 (d, $J = 6.5$ Hz, 8H, Ph-*H*), 7.40 (br, 12H, Ph-*H*), 7.15 (s, 4H, Ar-*H*), 4.30 (m, 12H, C*H*, Ph-CH_2), 4.05 (br, 8H, Ar-CH_2-N), 2.12 (q, $J = 7.5$ Hz, 8H, CH_2), 1.25 (m, 8H, CH_2), 0.93 (t, $J = 7.3$ Hz, 12H, CH_3); ^{13}C NMR (126 MHz, 30°C, $CDCl_3$) δ: 150.2, 130.5, 129.6, 129.5, 129.0, 126.3, 124.7, 108.6, 52.0, 42.1, 34.8, 33.8, 20.8, 13.9.

16b

Tetrabenzoxazine **9** (1.0 g, 0.84 mmol), 50 ml BuOH, 4 ml conc. HBr, 4 ml H_2O. Yield 0.52 g, 42%. Mp > 300°C (found C, 58.88; H, 6.12; N, 3.19. $C_{72}H_{88}N_4O_8Br_4 \cdot 0.25CHCl_3 \cdot 1.0CH_3CH_2CH_2OH$ requires C, 58.67; H, 6.34; N, 3.59) [$C_{72}H_{88}N_4O_8Br_4$ MW 1457.11; ESI-TOF MS [M-4Br-3H]$^+$1133.88]. ^{1}H NMR (500 MHz, $CDCl_3$, 30°C) δ: 8.90 (br, 8H, Ar-O*H*), 7.79 (d, $J = 6.5$ Hz, 8H, Ph-*H*) 7.74 (br, 8H, N-*H*), 7.45 (br, 12H, Ph-*H*), 7.18 (s, 4H, Ar-*H*), 4.43 (br, 8H, Ph-CH_2), 4.27 (t, $J = 7.8$ Hz, 4H, C*H*), 4.04 (br, 8H, Ar-CH_2-N), 2.13 (m, 8H, CH_2), 1.26 (m, 8H, CH_2), 0.92 (t, $J = 7.3$ Hz, 12H, CH_3); ^{13}C NMR (126 MHz, 30°C, $CDCl_3$) δ: 149.9, 130.8, 129.8, 129.2, 128.9, 125.9, 125.0, 107.8, 52.0, 42.4, 34.6, 33.7, 20.9, 13.8.

X-ray crystallography

Suitable single crystals for X-ray analysis were obtained by slow evaporation of resorcinarenes in the following solvent mixtures: **11a**–acetonitrile/dichloromethane; **11b** and **13b**–acetonitrile/dichloromethane/butanol; **12b**, **13aW**, **13aB**–butanol/methanol; **17a**–butanol/chloroform. Data were collected on a Bruker-Nonius Kappa Apex II diffractometer using graphite-monochromated Mo K_α radiation ($\lambda = 0.71073$ Å) at 123.0(1) K for **11a**, **12b**, **13aW**, **13aB** and **13b**, and at 173.0(1) K for **17a**. For **11b**, data were collected on the same instrument using graphite-monochromated Cu K_α radiation ($\lambda = 1.54184$ Å) at 123(2) K. *COLLECT* (*14*) software was used for the data collection and *DENZO-SMN* (*15*) for the data processing. The intensities were corrected for absorption using the multi-scan absorption correction method (*16*). The crystal structures of **11b**, **12b**, **13aB** and **13b** were solved by direct methods using *SIR*2002 (*17*), for the crystal structures of **13aW** and **17a** *SIR*97 (*18*) was used, and for structure solution of compound **11a** *SIR*2004 (*19*) program was used. All non-hydrogen atoms were refined anisotropically by full-matrix least-squares calculations based on F^2 (*20*). All hydrogen atoms in cations and solvent molecules were included in calculated positions as riding atoms, with *SHELXL97* (*20*) defaults. The choice of hydrogen position of OH groups in cations, methanol molecule in **12b** and butanol molecules in **13aB** and **17a** is determined by best hydrogen bond that can be created to an oxygen atom or halide ion. Hydrogen atoms of water molecules in **11b**, **13aW**, **13aB** and **13b** are modelled in a similar manner, with hydrogen atoms' coordinates kept fixed during refinement. The hydrogen atoms were not modelled for

Downloaded At: 14:39 29 January 2011

one half of the water molecule in **13b**, in which oxygen atom lies in special position. Disordered atoms in **11a** were refined freely with the following occupancy ratio: 0.689(8)/0.311(8) for the C41A and C42A atoms, 0.685(11)/0.315(11) for the C52A atom and 0.581(11)/0.419(11) for the C56A atom. In this structure, the C4 atom of one dichloromethane molecule is also disordered over two sites and is refined with a fixed occupancy ratio of 0.80/0.20. Two components, C41 and C42, could not be refined anisotropically satisfactorily, and therefore are refined only isotropically. In **11b**, disordered Br4 and C54 atoms were refined with fixed occupancy factors in 0.75/0.25 and 0.50/0.50 ratio, respectively, and the C82 and C83 atoms in **17a** with fixed occupancy factors in 0.50/0.50 ratio. The C44 and C45 atoms in **13b** are severely disordered. Although restraints were used in their refinement, they could not be modelled as disordered atoms and are refined only isotropically. Restraints on anisotropic displacement parameters were applied during the refinement of disordered atoms and several other atoms of **11a**, **11b**, **13aW**, **13b** and **17a**, and some geometrical restraints were used in the refinement of **11b**, **13aB**, **13b** and **17a**. Structures of **11b**, **12b**, **13aW**, **13aB**, **13b** and **17a** contain solvent-accessible voids with a small amount of solvent molecule(s) used for recrystallisation. As they could not be modelled satisfactorily, data were treated with the SQUEEZE routine in *PLATON* (*21*). High residual electron densities were observed for **11b** (1.961 e $Å^{-3}$, 2.40 Å from Br4) and **13aB** (2.490 e $Å^{-3}$, 1.01 Å from Cl4). Details of crystal data, data collection and refinement parameters are given in Table 2. *PLATON* (*21*) and *Mercury* (*22*) programs were used for structure analysis and drawing preparation. CCDC 776222–776228 contain the supplementary crystallographic data for this paper. These data can be obtained free of charge from The Cambridge Crystallographic Data Centre via www.ccdc.cam.ac.uk/data_request/cif.

Downloaded At: 14:39 29 January 2011

Supporting Information

Supporting Information data containing mass spectrometric analysis of **11a**, **11b** and **14a** (see Figures S1–S3) and tables with hydrogen-bonding geometries for compounds **11a**, **11b**, **12b**, **13aW**, **13aB**, **13b** and **17a** (see Tables S1–S7) are available via http://www.informaworld.com/gsch.

Acknowledgements

The authors gratefully acknowledge the financial support from the Academy of Finland (K.R., proj. 212588 and 218325) and the University of Jyväskylä (K.B. and K.R., academy professorship grant). M.C. is grateful to K.R., University of Zagreb and University of Jyväskylä for giving him an opportunity to work in his research group.

References

(1) (a) Timmerman, P.; Verboom, W.; Reinhoudt, D. *Tetrahedron* **1996**, *52*, 2663–2704. (b) Jasat, A.; Sherman, J.C. *Chem. Rev.* **1999**, *99*, 931–967.

(2) (a) Atwood, J.L.; Koutsantonis, G.A.; Raston C.L. *Nature* **1994**, *368*, 229–231. (b) Orr, G.W.; Barbour, L.J.; Atwood, J.L. *Science* **1999**, *285*, 1049–1052. (c) Atwood, J.L.; Barbour, L.J.; Jerga, A. *Science* **2002**, *296*, 2367–2369.

(3) (a) Schmidt, C.; Straub, T.; Falabu, D.; Paulus, E., Wegelius, E.; Kolehmainen, E.; Böhmer, V.; Rissanen, K.; Vogt. W. *Eur. J. Org. Chem.* **2000**, *23*, 3937–3944. (b) Steed, J.W.; Atwood, J.L. *Supramolecular Chemistry;* Wiley: Chichester, 2000. (c) Shivanyuk, A.; Rebek, J., Jr. *Chem. Commun.* **2001**, 2424–2425. (d) Luostarinen, M.; Shivanyuk, A.; Rissanen, K. *Org. Lett.* **2001**, *3*, 4141–4144. (e) Atwood, J.L.; Szumna, A. *J. Am. Chem. Soc.* **2002**, *124*, 10646–10647. (f) Luostarinen, M.; Partanen, T.; Schalley, C.A.; Rissanen, K. *Synthesis* **2004**, *2*, 255–262. (g) Strandman, S.; Luostarinen, M.; Niemelä, S.; Rissanen, K.; Tenhu, H. *J. Polym. Sci. Part A* **2004**, *42*, 4189–4201. (h) Nummelin, S.; Falabu, D.; Shivanyuk, A.; Rissanen, K. Org. Lett. **2004**, *6*, 2869–2872. (i) Luostarinen, M.; Åhman, A.; Nissinen, M.; Rissanen, K. *Supramol. Chem.* **2004**, *16*, 505–512. (j) Åhman, A.; Luostarinen, M.; Schalley, C.A.; Nissinen, M.; Rissanen, K. *Eur. J. Org. Chem.* **2005**, *13*, 2793–2801. (k) Beyeh, N.K.; Fehér, D.; Luostarinen, M.; Schalley, C.A.; Rissanen, K. *J. Incl. Phenom. Macrocyclic Chem.* **2006**, *56*, 381–394. (l) Beyeh, N.K.; Aumanen, J.; Åhman, A.; Luostarinen, M.; Mansikkamäki, H.; Nissinen, M.; Korppi-Tommola, J.; Rissanen, K. *New J. Chem.* **2007**, *31*, 370–376. (m) Luostarinen, M.; Nissinen, M.; Lähteenmäki, H.; Mansikkamäki, H.; Salorinne, K.; Schalley, C.A.; Rissanen, K. *J. Incl. Phenom. Macrocyclic Chem.* **2007**, *58*, 71–80.

(4) (a) Rudkevich; D.; Rebek, J., Jr. *Eur. J. Org. Chem.* **1999**, 1991–2005. (b) Atwood, J.L.; Szumna, A. *J. Supramol. Chem. 2.* **2002**, 479–482. (c) Nissinen, M.; Wegelius, E.; Falabu, D.; Rissanen, K. *CrystEngComm.* **2000**, *28*, 1–3. (d) Vuorimaa, E.; Vuorinen, T.; Tkachenko, N.; Cramariuc, O.; Hukka, T.; Nummelin, S.; Shivanyuk, A.; Rissanen, K.; Lemmetyinen, H. *Langmuir* **2001**, *17*, 7327–7331. (e) Falábu, D.; Shivanyuk, A.; Nissinen, M.; Rissanen, K. *Org. Lett.* **2002**, *4*, 3019–3022. (f) Nissinen, M.; Rissanen, K. *Supramol. Chem.* **2003**, *15*, 581–590.

(5) (a) Murayama, K.; Aoki, K. *Chem. Commun.* **1997**, *1*, 119–120. (b) Shivanyuk, A.; Rissanen, K.; Kolehmainen, E. *Chem. Commun.* **2000**, *13*, 1107–1108. (c) Shivanyuk, A.; Paulus, E.F.; Rissanen, K.; Kolehmainen, E.; Böhmer, V. *Chem. Eur. J.* **2001**, *7*, 1944–1951. (d) Mansikkamäki, H.; Nissinen, M.; Rissanen, K.; *Chem. Commun.* **2002**, 1902–1903. (e) Mansikkamäki, H.; Nissinen, M.; Schalley, C.A.; Rissanen, K. *New. J. Chem.* **2003**, *27*, 88–97. (f) Mansikkamäki, H.; Schalley, C.A.; Nissinen, M.; Rissanen, K. *New J. Chem.* **2005**, *29*, 116–127. (g) Mansikkamäki, H.; Nissinen, M.; Rissanen, K. *CrystEngComm.* **2005**, *7*, 519–526. (h) Åhman, A.; Luostarinen, M.; Rissanen, K.; Nissinen, M. *New. J. Chem.* **2007**, *31*, 169–177. (i) Beyeh, N.K.; Valkonen, A.; Rissanen, K. *Supramol. Chem.* **2009**, *21*, 142–148.

(6) (a) MacGillivray, L.R.; Atwood, J.L. *Nature* **1997**, *389*, 469–472. (b) Gerkensmeier, T.; Iwanek, W.; Agena, C.; Frölich, R.; Kotila, S.; Naher, C.; Mattay, J. *Eur. J. Org. Chem.* **1999**, 9, 2257–2262. (c) Atwood, J.L.; Barbour, L.J.; Jerga, A. *Chem. Commun.* **2001**, 2376–2377. (d) Rissanen, K. *Angew. Chem., Int. Ed. Eng.* **2005**, *44*, 3652–3654. (e)

Beyeh, N.K.; Kogej, M.; Åhman, A.; Rissanen, K.; Schalley, C.A. *Angew. Chem. Int. Ed.* **2006**, *45*, 5214–5218.
(7) (a) Mansikkamäki, H.; Nissinen, M.; Rissanen, K. *Angew. Chem. Int. Ed. Eng.* **2004**, *43*, 1263–1266. (b) Mansikkamäki, H.; Busi, S.; Nissinen, M.; Åhman, A.; Rissanen, K. *Chem. Eur. J.* **2006**, *12*, 4289–4296.
(8) Atwood, J.L.; Barbour, L.J.; Jerga, A.; Schottel, B.L. *Science* **2002**, *298*, 1000–1002.
(9) Zhu, S.S.; Staats, H.; Brandhorst, K.; Grunenberg, J.; Gruppi, F.; Dalcanale, E.; Lutzen, A.; Rissanen, K.; Schalley, C.A. *Angew. Chem. Int. Ed.* **2008**, *47*, 788–792.
(10) (a) Iwanek, W.; Mattay, J. *Liebigs Ann. Chem.* **1995**, 1463–1466. (b) Airola, K.; Böhmer, V.; Paulus, E.F.; Rissanen, K.; Schmidt, C; Thondorf, I.; Vogt, W. *Tetrahedron* **1997**, *53*, 10709–10724. (c) Airola, K.; Böhmer, V.; Paulus, E.F.; Rissanen, K.; Schmidt, C.; Thondorf, I.; Vogt, W. *Tetrahedron* **1997**, *53*, 10709–10724. (d) Schmidt, C.; Thondorf, I.; Kolehmainen, E.; Böhmer, V.; Vogt, W.; Rissanen, K. *Tetrahedron Lett.* **1998**, *39*, 8833–8836. (e) Beyeh, N.K.; Valkonen, A.; Rissanen, K. *Org. Lett.* **2010**, *12*, 1392–1395.
(11) (a) Shivanyuk, A.; Spaniol, T.P.; Rissanen, K.; Kolehmainen, E.; Böhmer, V. *Angew. Chem. Int. Ed.* **2000**, *39*, 3497–3500. (b) Luostarinen, M.; Nissinen, M.; Nieger, M.; Shivanyuk, A.; Rissanen, K. *Tetrahedron* **2007**, *63*, 1254–1263. (c) Far, A.R; Shivanyuk, A.; Rebek, J., Jr. *J. Am. Chem. Soc.* **2002**, *24*, 2854–2855.
(12) (a) Szumna, A. *Chem. Eur. J.* **2009**, *15*, 12381–12388. (b) Szumna, A. *Chem. Commun.* **2009**, 4191–4193. (c) Kuberski, B.; Szumna, A. *Chem. Commun.* **2009**, 1959–1961.
(13) Mäkinen, M.; Holopainen, S.; Rissanen, K.; Vainiotalo, P. *Rapid Commun. Mass Spectrom.* **2006**, *20*, 1082–1086.
(14) Hooft, R.W.W. *COLLECT*; Nonius BV: Delft, The Netherlands, 1998.
(15) Otwinowski, Z.; Minor, W. Processing of X-ray Diffraction Data Collected in Oscillation Mode. In *Methods in Enzymology, Vol. 276: Macromolecular Crystallography, Part A*; Carter, C.W., Jr., Sweet, R.M., Eds.; Academic Press: New York, 1997.
(16) Sheldrick, G.M. *SADABS 2008/2*; University of Göttingen: Göttingen, Germany, 2008.
(17) Burla, M.C.; Camalli, M.; Carrozzini, B.; Cascarano, G.L.; Giacovazzo, C.; Polidori, G.; Spagna, R. *J. Appl. Crystallogr.* **2003**, *36*, 1103.
(18) Altomare, A.; Burla, M.C.; Camalli, M.; Cascarano, G.L.; Giacovazzo, C.; Guagliardi, A.; Moliterni, A.G.G.; Polidori, G.; Spagna, R. *J. Appl. Crystallogr.* **1999**, *32*, 115–119.
(19) Burla, M.C.; Caliandro, R.; Camalli, M.; Carrozzini, B.; Cascarano, G.L.; De Caro, L.; Giacovazzo, C.; Polidori, G.; Spagna, R. *J. Appl. Crystallogr.* **2005**, *38*, 381–388.
(20) Sheldrick, G.M. *Acta Crystallogr.* **2008**, *A64*, 112–122.
(21) Spek, A.L. *J. Appl. Crystallogr.* **2003**, *36*, 7–13.
(22) Macrae, C.F.; Edgington, P.R.; McCabe, P.; Pidcock, E.; Shields, G.P.; Taylor, R.; Towler, M.; van de Streek, J. *J. Appl. Crystallogr.* **2006**, *39*, 453–457.

Downloaded At: 14:39 29 January 2011